ρN resonance dynamics in the proton nucleus reaction

Swapan Das
Nuclear Physics Division, Bhabha Atomic Research Centre,
Mumbai-400 085, India

January 18, 2011

Abstract

The strong coupling of rho meson to the nucleon produces s and p wave rho meson nucleon (ρN) resonances. In a nucleus, the ρN resonance-hole polarization generates the optical potential or self-energy for the rho meson. The scattering of rho meson due to this potential provides valuable informations about the ρN resonance dynamics in a nucleus. To investigate it, we use this potential to calculate the mass distribution spectrum for the ρ meson produced coherently in the proton nucleus reaction. The cross sections arising due to s and p wave ρN resonances have been presented. The coherent and incoherent contributions to the cross sections due to these resonances are compared. In addition, the calculated results due to non-relativistic and relativistic ρ meson self-energy are illustrated.

PACS number(s): 25.40.Ve, 24.30.-v, 24.50.+g

Key words: Proton-nucleus reaction, ρ meson-nucleon resonance dynamics, ρ meson production

1 INTRODUCTION

The rho meson nucleon resonances arise because of the strong coupling of this meson to the nucleon. The importance of the hadronic resonances in the particle production phenomena is undoubtedly understood from long ago. For example, the pion production data in the nuclear reaction below 1 GeV had been interpreted successfully by the formation of the $\Delta(1232)$ resonance in the intermediate state [1]. Therefore, the dynamics of the ρN resonances can have intimate relationship with the rho meson production in the nuclear reaction. The sub-threshold rho meson emission is well described by the $N(1520)$ resonance production in the intermediate state [2]. At higher energy, the importance of $N(1720)$ resonance has been discussed [3] in context to the ρ meson production in the

proton nucleus reaction. Therefore, the study of the rho meson production in the nuclear reaction can unveil many interesting physics of the ρN resonance dynamics in a nucleus.

The ρN resonances were also found significant to investigate the modification of the rho meson in the nuclear medium. Sometime back, Kondratyuk et al., [4] estimated the rho meson nucleon scattering amplitude, i.e., $f_{\rho N}$, due to the formation of ρN resonances in the intermediate state. Using this amplitude, they have shown the ρ meson mass in a nucleus is below 770 MeV in the static limit. This agrees with the result of scaling hypothesis formulated by Hatsuda and Lee [5]. Friman et al., [6] calculated the ρ meson self-energy arising due to p wave ρN scattering, via $N(1720)$ and $\Delta(1905)$ resonances. According to their calculation, this self-energy (which appears in the ρ meson spectral function) reduces the mass of the ρ meson at high baryon density. Peters et al., [7] extended this calculation by incorporating contributions from all four starred s and p wave ρN resonances. As shown by them, the s wave ρN resonances (specifically, $N(1520)$) have significant influence on the ρ meson spectral function. The ρ meson self-energy due to s wave ρN resonance-hole polarization shows an important feature, as it depends upon both energy and momentum of the rho meson. Therefore, the self-energy due to s wave ρN resonance can contribute to the ρ meson spectral function in the static limit. This is unlike to that occurring due to p wave ρN scattering, where the rho meson self-energy depends only on its momentum.

The self-energy or optical potential is inevitable to describe the elastic scattering of a particle by the nucleus. Using it, we studied various aspects for the coherent (elastic) scattering of ρ^0 meson in the proton nucleus reaction [8]. In one part of this study, we investigated the sensitivity of the coherent ρ^0 meson mass distribution on its optical potential formulated by various authors [4, 5, 6, 9] including Peters et al., [7]. The later authors, as mentioned above, have shown non-relativistically that various ρN resonances can generate the self-energy for the rho meson in a nucleus. Due to lack of scope, we could not show in our earlier work [8] the distinct contribution arising from each ρN resonance to the ρ^0 meson production cross section. Therefore, those are illustrated in the present work. In addition, we extend our calculation to accommodate the relativistic evaluation of the ρ meson self-energy due to these resonances and discuss how the ρN resonance behave relativistically in the above reaction. We compare the non-relativistic and relativistic optical potentials for the ρ^0 meson arising due to each ρN resonance-hole polarization in the nucleus. We also present the results for the coherent and incoherent contributions of these resonances to the overall cross sections.

2 FORMALISM

The coherent ρ^0 meson production in the proton nucleus reaction describes the elastic scattering of the virtual rho meson (emitted by the beam proton) to its real state. Symbolically, this reaction is used to express as $p + A(\text{g.s.}) \rightarrow p' + \rho^0 + A(\text{g.s.})$. As we worked out earlier [8], the double differential cross section for the coherent ρ meson mass

distribution in the (p, p') reaction on a nucleus is given by

$$\frac{d\sigma}{dm d\Omega_{p'}} = \int\int d\Omega_\rho dE_{p'} [KF] S(m^2) < |T_{fi}|^2 >, \tag{1}$$

where $[KF]$ is the kinematical factor associated with this reaction. The expression for it is

$$[KF] = \frac{m_p^2 E_{A'}}{(2\pi)^5} \frac{k_{p'} k_\rho^2 m}{k_p |k_\rho (E_i - E_{p'}) - (\mathbf{k}_p - \mathbf{k}_{p'}) \cdot \hat{k}_\rho E_\rho|}. \tag{2}$$

The factor $S(m^2)$ in Eq. (1) denotes the mass distribution function for the rho meson of mass m in the free space. It is well addressed by the Breit-Wigner form [10]:

$$S(m^2) = \frac{1}{\pi} \frac{m_\rho \Gamma_\rho(m^2)}{[(m^2 - m_\rho^2)^2 + m_\rho^2 \Gamma_\rho^2(m^2)]}, \tag{3}$$

with $m_\rho (\simeq 770$ MeV) being the resonance mass of the ρ meson in the free state. $\Gamma_\rho(m^2)$ represents the total free space decay width for the ρ meson of mass m, arising dominantly ($\sim 100\%$) due to $\rho^0 \to \pi^+\pi^-$. Therefore, $\Gamma_\rho(m^2)$ can be written as

$$\Gamma_\rho(m^2) \approx \Gamma(m_\rho^2)_{\rho\to\pi\pi} \left(\frac{m_\rho}{m}\right) \left[\frac{k(m^2)}{k(m_\rho^2)}\right]^3 \Theta(m^2 - 4m_\pi^2), \tag{4}$$

with $\Gamma(m_\rho^2)_{\rho\to\pi\pi} \approx 150$ MeV. $k(m^2)$ is the pion momentum in the rest frame of decaying ρ^0 meson of mass m. This expression intrinsically implies the detection of rho meson through its decay products $\pi^+\pi^-$ in the final state. We have not considered here the distortion due to pion nucleus scattering since the effect of it (in this kind of reaction) has been found insignificant [11].

T_{fi} in Eq. (1) is the T-matrix for the coherent rho meson production in the proton nucleus reaction. The annular bracket around $|T_{fi}|^2$ represents the average and summation over spins and polarization of the initial and final states respectively. T_{fi} is given by

$$T_{fi} = \int\int d\mathbf{r}' d\mathbf{r}\ \chi^{(-)*}(\mathbf{k}_\rho, \mathbf{r}') \Pi_\rho(\mathbf{r}') G_\rho(\mathbf{r}' - \mathbf{r}) \Psi_\rho(\mathbf{q}, \mathbf{r}). \tag{5}$$

In this equation, $G_\rho(\mathbf{r}' - \mathbf{r})$ describes the propagation of the virtual ρ^0 meson from $\mathbf{r}$ to $\mathbf{r}'$, where the elastic scattering of this meson (to its real state) is taken place due to the ρ meson nucleus optical potential $V_{O\rho}(\mathbf{r}')$. This potential appears in the above equation through the ρ meson self-energy, i.e., $\Pi_\rho(\mathbf{r}') = 2q_0 V_{O\rho}(\mathbf{r}')$. Here, $q_0 (= E_p - E_{p'})$ is the energy of the virtual rho meson. $\Pi_\rho(\mathbf{r}')$ will be elaborated in the next section.

The symbol $\Psi_\rho(\mathbf{q}, \mathbf{r})$ in Eq. (5) stands for the virtual rho meson production amplitude in the (p, p') reaction. The expression for it is

$$\Psi_\rho(\mathbf{k}_{p'}, \mathbf{k}_p; \mathbf{r}) = \chi^{(-)*}(\mathbf{k}_{p'}, \mathbf{r}) \Gamma_{\rho NN} \chi^{(+)}(\mathbf{k}_p, \mathbf{r}), \tag{6}$$

where $\Gamma_{\rho NN}$ denotes the vertex function at the $\rho^0 pp'$ vertex. It is governed by the ρNN Lagrangian as described in Ref. [8]. χs represent the distorted wave functions for protons

in the continuum. In the energy region of ρ meson production, the distortion arising due to proton nucleus scattering is purely absorptive. Therefore, the distorted wave functions for protons can be approximated by their plane waves multiplied by the attenuation factor $\mathcal{A}_{\mathcal{F}}$ for them [12], i.e.,

$$\chi^{(-)*}(\mathbf{k}_{p'}, \mathbf{r})\chi^{(+)}(\mathbf{k}_p, \mathbf{r}) \approx \mathcal{A}_{\mathcal{F}} e^{i\mathbf{q}.\mathbf{r}}; \qquad \mathbf{q} = \mathbf{k}_p - \mathbf{k}_{p'}. \tag{7}$$

This equation shows $\mathbf{q}$ is the momentum of the virtual rho meson emitted at the ρNN vertex.

The ρ^0 meson in the final state can emit in all directions. Therefore, the partial wave expansion is preferred to express its wave function $\chi^{(-)}(\mathbf{k}_\rho, \mathbf{r}')$ appearing in Eq. (5), i.e.,

$$\chi^{(-)*}(\mathbf{k}_\rho, \mathbf{r}) = \frac{4\pi}{k_\rho r} \sum_{lm} (-i)^l u_l(k_\rho r) Y^*_{lm}(\hat{k_\rho}) Y_{lm}(\hat{r}). \tag{8}$$

The radial part of this wave function, i.e., $u_l(k_\rho r)$, is generated by solving the relativistic wave (Schrödinger) equation using the ρ meson optical potential $V_{O\rho}(\mathbf{r})$, described later.

3 RESULTS AND DISCUSSION

The attenuation factor $\mathcal{A}_{\mathcal{F}}$ in Eq. (7), which accounts the distortion for protons, can be estimated by using the following equation [12]:

$$\mathcal{A}_{\mathcal{F}} = \frac{1}{A} \int d\mathbf{b} T(\mathbf{b}) exp[-Im\delta(\mathbf{b})], \tag{9}$$

where A is the mass number of the nucleus. $T(\mathbf{b})[= \int_{-\infty}^{+\infty} \varrho(\mathbf{b}, z)dz]$ represents the thickness function for the nucleus at the impact parameter $\mathbf{b}$. $\varrho(\mathbf{b}, z)$ describes the density distribution for the nucleus, given in Eq. (12) for ^{12}C nucleus. $\delta(\mathbf{b})$ denotes the total phase shift function for the proton nucleus scattering, i.e., $\delta(\mathbf{b}) = \delta_p(\mathbf{b}) + \delta_{p'}(\mathbf{b})$. The form for it is given by

$$\delta_p(\mathbf{b}) = -\frac{1}{v_p} \int_0^\infty V_{Op}(\mathbf{b}, z)dz, \tag{10}$$

where v_p is the velocity of the proton. $V_{Op}(\mathbf{b}, z)$ denotes the optical potential for the proton nucleus scattering.

The imaginary part of the proton nucleus optical potential $V_{Op}(\mathbf{b}, z)$ is required to evaluate the attenuation factor $\mathcal{A}_{\mathcal{F}}$ for protons (see Eqs. (9) and (10)). Using the high energy ansatz, i.e., "$t\varrho$" approximation, the imaginary part of $V_{Op}(\mathbf{b}, z)$ can be written as

$$ImV_{Op}(\mathbf{r}) = -\frac{1}{2} v \sigma_t^{pN} \varrho(\mathbf{r}). \tag{11}$$

v is the relative velocity in the proton nucleon cm system. σ_t^{pN} denotes the total cross section for the proton nucleon scattering. The energy dependent values for it is taken

from the measurements [13, 14]. $\varrho(\mathbf{r})$ describes the spatial shape of the optical potential $V_{Op}(\mathbf{r})$. It is usually approximated by the density distribution of the nucleus. The form of $\varrho(\mathbf{r})$ for the ^{12}C nucleus, as extracted from the electron scattering data [15], is given by

$$\varrho(\mathbf{r}) = \varrho_0[1 + w(r/c)^2]e^{-(r/c)^2}; \quad w = 1.247, \; c = 1.649 \text{ fm}. \tag{12}$$

This density is normalized to the mass numbers of the nucleus.

As mentioned earlier, we look for the contribution of the individual ρN resonance to the cross section for the coherent rho meson production in the proton nucleus reaction. Upto $\sim$ 1.9 GeV, the existence of these resonances (which emit ρ meson) is confirmed [14]. The formation of these resonances in a nucleus generates the ρN resonance-hole polarizations in it. The interaction energy associated with these polarizations is referred as the self-energy or optical potential for the rho meson. This potential can modify the ρ meson propagation through the nucleus. Therefore, the ρ meson production process in the nuclear reaction can be thought as a potential tool to investigate the ρN resonance dynamics in a nucleus.

To disentangle the above issue explicitly, we use the rho meson self-energy (or optical potential) evaluated by Peter et al., [7]. According to them, the ρ meson self-energy due to s wave (negative parity) ρN resonance is given by

$$\Pi^{\mu\nu}_{(s)}(k_0, \mathbf{k}) = -(k_0^2 P_T^{\mu\nu} - k^2 P_L^{\mu\nu}) \left(\frac{f_{RN\rho}}{m_\rho}\right)^2 F'(\mathbf{k}^2) S_\Sigma \beta(k_0, \mathbf{k}), \tag{13}$$

with $k^2 = k_0^2 - \mathbf{k}^2$. k_0 and $\mathbf{k}$ are the energy and momentum respectively of the rho meson. $F'(\mathbf{k}^2)$ is the monopole form factor associated with the ρ meson self-energy: $F'(\mathbf{k}^2) = \frac{\Lambda'^2}{\Lambda'^2 + \mathbf{k}^2}$ with $\Lambda' = 1.5$ GeV [7]. $P_T^{\mu\nu}$ and $P_L^{\mu\nu}$ denote the respective longitudinal and transverse projection operators for the self-energy. They are normalized as $P_L^{\mu\nu} P_{\mu\nu L} = 1$ and $P_T^{\mu\nu} P_{\mu\nu T} = 2$. The longitudinal and transverse self-energies can be obtained by using following relations [7]:

$$\Pi_L^{(s)}(k_0, \mathbf{k}) = -P_L^{\mu\nu} \Pi_{\mu\nu}(k_0, \mathbf{k}); \qquad \Pi_T^{(s)}(k_0, \mathbf{k}) = -\frac{1}{2} P_T^{\mu\nu} \Pi_{\mu\nu}(k_0, \mathbf{k}). \tag{14}$$

The average ρ meson self-energy due to s wave ρN resonances is given by $\Pi^{(s)}(k_0, \mathbf{k}) = \frac{1}{3}[2\Pi_T^{(s)}(k_0, \mathbf{k}) + \Pi_L^{(s)}(k_0, \mathbf{k})]$. On the other hand, the ρ meson self-energy due to p wave (positive parity) ρN resonance is purely transverse. The expression for it [7] is

$$\Pi^{(p)}(k_0, \mathbf{k}) \equiv \Pi_T^{(p)}(k_0, \mathbf{k}) = \mathbf{k}^2 \left(\frac{f_{RN\rho}}{m_\rho}\right)^2 F'(\mathbf{k}^2) S_\Sigma \beta(k_0, \mathbf{k}). \tag{15}$$

In Eqs. (13) and (15), $f_{RN\rho}$ denotes the constant for the rho meson-nucleon coupling to the resonance R, and S_Σ represents the associated spin-isospin transition factor. As shown by Peters et al. [7], there are four s-wave ρN resonances, namely $N(1520)$, $\Delta(1620)$, $N(1650)$, $\Delta(1700)$, and five p-wave ρN states $N(940)$, $\Delta(1232)$, $N(1680)$, $N(1720)$ and

$\Delta(1905)$. Values of $f_{RN\rho}$ and S_Σ for these resonances, as estimated by Peters et al. [7], are listed in the Table-1. For $\Delta(1232)$ resonance, the Landau-Migdal parameter g is introduced to account for the short-range correlation: $\Pi_\Delta^{(p)}(k_0,\mathbf{k}) \rightarrow \Pi_\Delta^{(p)} / \left[1 - g\frac{\Pi_\Delta^{(p)}}{k^2}\right]$, with $g = 0.5$. The inclusion of Landau-Migdal parameter for other resonances was not recommended [7]. The resonance $N(1440)$ was not incorporated in this calculation, since its width decaying to the ρN channel is insignificant ($8 < \%$).

The Linhard function $\beta(k_0,\mathbf{k})$ appearing in Eqs. (13) and (15) is given by

$$\beta(k_0,\mathbf{k}) = -\int_0^{p_F} \frac{d\mathbf{p}}{(2\pi)^3}\left[\frac{1}{k_0 - E_N(\mathbf{p}) + E_R(\mathbf{p}+\mathbf{k})} + \frac{1}{-k_0 - E_N(\mathbf{p}) + E_R(\mathbf{p}-\mathbf{k})}\right]. \quad (16)$$

This integration eventually means the summation over all nucleons, i.e., $\Sigma_i \rightarrow 4V\int_0^{p_F}\frac{d\mathbf{p}}{(2\pi)^3}$. $E_N(\mathbf{Q})$ and $E_R(\mathbf{Q})$ represent energies for the nucleon N and resonance R respectively. They are defined as

$$E_N(\mathbf{Q}) = \sqrt{m_N^2 + \mathbf{Q}^2}; \qquad E_R(\mathbf{Q}) = \sqrt{m_R^2 + \mathbf{Q}^2} - \frac{i}{2}\Gamma_R, \quad (17)$$

where Γ_R denotes the width of the resonance R. It is composed of the pion-nucleon and rho meson-nucleon decay widths, i.e., $\Gamma_R = \Gamma_{R\rightarrow N\pi} + \Gamma_{R\rightarrow N\rho}$, elaborated in the Ref. [7].

In the non-relativistic calculation done by Peters et al. [7], the ρ meson self-energies (given in Eqs. (13) - (15)) were evaluated in the nucleon rest frame except the coupling constant $f_{RN\rho}$ appearing in it. This constant was calculated in the resonance rest frame. In the nucleon rest frame, the Linhard function $\beta(k_0,\mathbf{k})$ in Eq. (16) is reduced to

$$\beta(k_0,\mathbf{k}) = \frac{1}{2}\varrho\frac{E_R(\mathbf{k}) - m_N}{k_0^2 - [E_R(\mathbf{k}) - m_N]^2}. \quad (18)$$

In this case, k is the four momentum of the ρ meson in the nucleon rest frame. In fact, this is the expression for $\beta(k_0,\mathbf{k})$ normally used in the nuclear matter calculation in the limit of low nuclear density ϱ or high momentum $|\mathbf{k}| \gg p_F$. The rho meson optical potential obtained from its self-energy, i.e., $V_{O\rho} = \frac{1}{2k_0}\Pi_\rho$, is transformed in the proton nucleus cm system using proper kinematics. The radial density distribution ϱ for the ^{12}C nucleus is expressed in the Eq. (12).

Using the ρ meson self-energy described above, we calculate the mass distribution spectra for the coherent rho meson produced in the (p,p') reaction on ^{12}C nucleus. The beam energy for this reaction is taken equal to 3.5 GeV, and the ejectile p' emission angle is taken fixed at 1^0. In Fig. 1, the cross sections arising due to s wave ρN resonances are presented, and those due to p wave ρN resonances are shown in Fig. 2. It is noticeable in these figures that the cross sections due to p wave ρN resonances are much larger than those due to the s wave ρN resonances. In addition, these figures also show that all s wave or p wave ρN resonances do not contribute identically to the cross section. It occurs since the cross section of this reaction depends upon various quantities, such

as coupling constant $f_{RN\rho}$, spin-isospin factor S_Σ, hadron parameters for the resonance, ... etc. These quantities, as mentioned earlier, are listed in Table-1 for all resonances. Remarkably, the magnitude of the cross section strongly depends on the resonance(R)-rho meson(ρ)-nucleon(N) coupling constant $f_{RN\rho}$. As shown in Table-1, $f_{RN\rho}$ for the p wave ρN resonances are relatively larger. They lie within the range 6.3 to 15.3, whereas $f_{RN\rho}$ for the s wave ρN resonances are within the range of 0.9 to 7.0. Therefore, the cross section due to p wave ρN resonance is expected to be larger than that due to s wave ρN resonance.

Fig. 1 shows that the ρ^0 meson production cross section due to $N(1520)$ resonance (solid curve (a)) is the largest compared to those originating due to other s wave ρN resonances. This resonance, as compared in Table-1, has the largest ρN coupling constant, i.e., $f_{RN\rho} = 7$. The spin-isospin factor S_Σ for it (equal to 8/3) is also quite significant. The peak cross section due to this resonance is found equal to 5.64 μb/(GeV sr), and it appears at 720 MeV in the ρ meson mass distribution spectrum. The second largest cross section distribution for the rho meson production, presented by the dot dot dashed curve (b), arises due to $\Delta(1700)$ resonance. This curve shows that the cross section at the peak is equal to 1.15 μb/(GeV sr), and the peak position appears at the ρ meson mass equal to 710 MeV. For this resonance, values for $f_{RN\rho}$ and S_Σ are equal to 5 and 16/9 respectively. The ρ meson production cross section due to $\Delta(1620)$ resonance (dashed curve (c)) is 0.37 μb/(GeV sr) at the peak, appearing at the ρ meson mass equal to 710 MeV. $f_{RN\rho}$ and S_Σ for $N(1620)$ are equal to 2.5 and 8/3 respectively. The ρ meson production cross section due to $N(1650)$ resonance (dotted curve (d), not properly visible in Fig. 1) is very small. It happens due to its weak coupling to the ρ meson and nucleon, i.e., $f_{RN\rho} = 0.9$. However, S_Σ for $N(1650)$ is significant (equal to 4).

The rho meson mass distribution spectra due to p wave ρN resonances, as mentioned earlier, are presented in Fig. 2. As shown in this figure, the maximum cross section arises due to $\Delta(1905)$ resonance (see dashed curve (a)). For this resonance, $f_{RN\rho}$ and S_Σ are equal to 12.2 and 4/5 respectively. The cross section at the peak is equal to 36.63 μb/(GeV sr), and it appears at the ρ meson mass equal to 640 MeV. The dot dot dashed curve (b) represents the second largest cross section distribution originating due to $\Delta(1232)$ isobar. This curve shows its peak at the ρ meson mass equal to 720 MeV, and the cross section at the peak is equal to 35.17 μb/(GeV sr). The constant $f_{RN\rho}$ for the $\Delta(1232)$ coupling to the ρ meson and nucleon is quite large. The magnitudes for $f_{RN\rho}$ and S_Σ for this resonance are equal to 15.3 and 16/9 respectively. It must be mentioned that $\Delta(1232)$ does not have measurable branching ratio into two pions. Therefore, the value of the $\Delta N\rho$ coupling constant, i.e., $f_{RN\rho}(\equiv f_{\Delta N\rho})$, can't be determined from the measured decay width. Since the magnitude of $f_{\Delta N\rho}$ is uncertain, the cross section arising due to $\Delta(1232)$ resonance can be interpreted only qualitatively. We have taken the above value of $f_{\Delta N\rho}$ since it is used by Peters et al., [7] to calculated the rho meson self-energy.

The ρ^0 meson production cross section due to $N(1720)$ resonance (shown by the solid curve (c)) in Fig. 2 is also significant. $f_{RN\rho}$ and S_Σ for this resonance are 7.8 and 8/3 respectively. The calculated spectrum due to this resonance shows a peak at the ρ

meson mass equal to 720 MeV, and the cross section at the peak is 31 μb/(GeV sr). The ρ^0 meson production cross section due to nucleon $N(940)$ is presented by the dot dashed curve (d) in Fig. 2. The ρNN coupling constant $f_{NN\rho}$ and S_Σ are taken equal to 7.7 and 4 respectively. This curve shows that the cross section at the peak is equal to 18.99 μb/(GeV sr) and the peak position appears at the ρ meson mass equal to 720 MeV. The cross section due to $N(1680)$ resonance (dotted curve (e)) is least compared to those due to other p wave ρN resonances. For this resonance, $f_{NN\rho}$ and S_Σ are equal to 6.3 and 6/5 respectively.

The coherent and incoherent addition of the cross sections due to all (s and p wave) ρN resonances have been compared in Fig. 3. The incoherent addition of the cross sections due to all ρN resonances (dot dashed curve) shows the cross section at the peak is equal to $\sim$ 0.126 mb/(GeV sr) and it appears at the ρ meson mass equal to 710 MeV. The peak cross section due to coherent contribution of all ρN resonances (solid curve) appears at 730 MeV in the ρ meson mass distribution spectrum, and its value is equal to 1.35 mb/(GeV sr). Therefore, the coherent addition increases the cross section drastically. It enhances the value of the cross section at the peak by a factor about 10.7 over that due to incoherent contribution. The peak position due to later appears 20 MeV higher in the ρ meson mass distribution spectrum.

The calculated results presented in Figs. 1$-$3 are based on the choice of the ρ meson self-energies (given in Eqs (13) - (18)) evaluated by Peters et al., [7]. As mentioned earlier, this is a preferable choice in the nuclear matter calculation. However, this choice had been criticized by Post et al. [16], since it leads serious uncertainty in the non-relativistic calculation. According to them, the ρ meson self-energies in Eqs. (13) and (15) also should be calculated in the resonance rest frame. This approach gives very reasonable agreement with the relativistic calculation for the rho meson self-energy [16]. Therefore, the calculated cross section using this approach can be considered as the relativistic results. Since the spectra appearing in Figs. 1$-$3 are due to the non-relativistic calculation for the ρ meson self-energy, we refer them henceforth as non-relativistic results. Another advantage of the resonance rest frame calculation is that the complicated relativistic calculation for the rho meson self-energy due to spin-$\frac{5}{2}$ ρN resonance can be avoided. In the resonance rest frame, the form for the Linhard function $\beta(k_0, \mathbf{k})$ in Eq. (16) can be simplified to

$$\beta(k_0, \mathbf{k}) = \frac{1}{2}\varrho \frac{m_R - \frac{i}{2}\Gamma_R - E_N(\mathbf{k})}{k_0^2 - [m_R - \frac{i}{2}\Gamma_R - E_N(\mathbf{k})]^2}, \tag{19}$$

where k is the four momentum of the ρ^0 meson in the resonance rest frame. All other quantities have been defined earlier.

To explore the relativistic effect on the cross section, we recalculate the ρ meson mass distribution spectra in the (p, p') reaction using the relativistic ρ meson nucleus optical potential illustrated above. The cross sections originating due to s wave ρN resonances are shown in Fig. 4. This figure looks qualitatively similar to the non-relativistic results presented in Fig. 1. It is noticeable that magnitudes of the cross sections in the relativistic

calculation have gone up significantly compared to those obtained in the non-relativistic case. Specifically, the enhancement in the cross section is found more than 3 times larger for the $N(1520)$ and $\Delta(1700)$ resonances. This enhancement occurs due to the increase in the rho meson potential, listed in Table-2, in the relativistic calculation.

The cross section due to $N(1520)$ resonance (solid curve (a) in Fig. 4) is distinctly largest in the relativistic case also. The peak in the calculated ρ meson mass distribution spectrum due to this resonance appears at 730 MeV, and the cross section at the peak is equal to 20.04 μb/(GeV sr). The second largest cross section for the rho meson mass distribution arises due to the $\Delta(1700)$ resonances (dot dot dashed curve (b)). The cross section at the peak is equal to 3.82 μb/(GeV sr), and the peak appears at the rho meson mass equal to 730 MeV. The dashed curve (c) represents the mass distribution spectrum for the rho meson due to the $\Delta(1620)$ resonance. The peak cross section for this distribution is equal to 0.70 μb/(GeV sr), and it appears at the ρ meson mass equal to 720 MeV. Similar to the non-relativistic case, the cross section due to $N(1650)$ resonance (dotted curve (d), not prominently seen in Fig. 4) is insignificant compared to those due to other s wave ρN resonances.

The calculated (relativistic) rho meson mass distribution spectra due to p wave ρN resonances are shown in Fig. 5. Unlike to the case of s wave ρN resonances, these spectra are not qualitatively similar to the non-relativistic results presented in Fig. 2. The ρ meson mass distribution spectra in Fig. 5 show that the largest cross section arises due to $\Delta(1232)$ resonance. The second largest cross section originates due to the $\Delta(1905)$ resonance. It is exactly opposite to the non-relativistic results (see in Fig. 2). We again mention that the cross section due to $\Delta(1232)$ resonance can be described only qualitatively, since uncertainty exists in determining the $\Delta N\rho$ coupling constant $f_{\Delta N\rho}$. We do not incorporate the cross section due to $N(940)$ in Fig. 5, since the relativistic calculation for it, as mentioned by Post et al. [16], leads huge over estimation of the elementary rho production (e.g., $\gamma N \to \rho N$ and $\pi N \to \rho N$) data. It is remarkable that the relativistic calculation for the p wave ρN resonance gives on an average about 67% less cross section compare to that due to non-relativistic calculation. This reduction occurs since the relativistic optical potential due to p wave ρN resonance-hole polarization, as presented in Table-2, is less than that due to non-relativistic calculation. This is in contrast to the s wave ρN resonance case.

The cross section distribution due to the $\Delta(1905)$ resonance is described by the dashed curve (a) in Fig. 5. It shows that the peak cross section is equal to 20.92 μb/(GeV sr), and the peak position appears at 650 MeV in the ρ meson mass distribution spectrum. The dot dot dashed curve (b) represents the ρ meson mass distribution spectrum arising due to the $\Delta(1232)$ resonance. This curve shows that the calculated cross section at the peak is equal to 26.84 μb/(GeV sr), and the peak appears at the rho meson mass equal to 720 MeV. The solid curve (c) illustrates the ρ meson mass distribution spectrum due to the $N(1720)$ resonance. The cross section due to it is equal to 19.68 μb/(GeV sr) at the peak, and it appears at the rho meson mass equal to 720 MeV. The cross section due to $N(1680)$ resonance (dotted curve (d)) is the smallest amongst those due to other p

wave ρN resonances. To be mentioned, the non-relativistic calculation corroborates this finding qualitatively.

The calculated relativistic results for the coherent and incoherent contributions to the cross section arising from all (s and p wave) resonances are compared in Fig. 6. The calculated cross sections in this case show features qualitatively similar to the non-relativistic results presented in Fig. 3. The incoherent addition of the cross sections due to all ρN resonances gives smaller cross section (dot dashed curve). It is equal to 0.11 mb/(GeV sr) at the peak, appearing at the ρ meson mass equal to 720 MeV. Whereas, the coherent contribution of all ρN resonances (solid curve) enhances the cross section by a factor about 7.82 to 0.86 mb/(GeV sr). The peak position in the later case appears at 730 MeV in the ρ meson mass distribution spectrum.

4 CONCLUSIONS

The ρ meson nucleon resonance dynamics in the nucleus have been studied through the coherent ρ^0 meson production process in the proton nucleus reaction. This study shows that the cross section strongly depends upon the ρ meson-nucleon-resonance coupling constant. It also depends on various other quantities, such as the spin-isospin transition factor and the hadron parameters for the resonance .... etc. The cross sections arising due to p wave ρN resonances are larger than those due to s wave ρN resonances. Amongst the s wave resonances, the largest cross section originates distinctly due to $N(1520)$ resonance. The relativistic results are qualitatively similar to the non-relativistic results in the case of s wave ρN resonances. The relativistic calculation for these resonances gives larger cross sections. These features are opposite in the case of p wave ρN resonances dynamics. The coherent contribution of all resonances enhances the cross section drastically over that due to incoherent contribution.

5 ACKNOWLEDGEMENTS

The author gratefully acknowledges A.K. Mohanty, R.K. Choudhury and S. Kailas.

References

[1] G. E. Brown and W. Weise, Phys. Rep. **22** 279 (1975); E. Oset, H. Toki and W. Weise, Phys. Rep. **83** 281 (1982); B. K. Jain and A. B. Santra Phys. Rep. **230** 1 (1993); T.-S. H. Lee and R. P. Redwine, Annu. Rev. Nucl. Part. Sci. **52** 23 (2002); T. E. O. Ericson and W. Weise, *Pions and Nuclei* (Clarendon Press, Oxford, 1988); Swapan Das, Phys. Rev. C **70** 034604 (2004).

[2] G. M. Huber et al., Phys. Rev. C **68** 065202 (2003); G. M. Huber, G. J. Lolos and Z. Papandreou, Phys. Rev. Lett. **80** 5285 (1998); G. J. Lolos et al., ibid. **80** 241 (1998).

[3] Swapan Das et al., Int. J. Mod. Phys. E **8** 243 (1999).

[4] L. A. Kondratyuk, A. Sibirtsev, W. Cassing, Ye. S. Golubeva and M. Effenberger, Phys. Rev. C **58**, 1078 (1998).

[5] T. Hatsuda and S.H. Lee, Phys. Rev. C **46**, R34 (1992).

[6] B. Friman, Nucl. Phys. **A610**, 358c (1996); B. Friman and H.J. Pirner, Nucl. Phys. **A617**, 496 (1997).

[7] W. Peters, M. Post, H. Lenske, S. Leupold and U. Mosel, Nucl. Phys. **A632**, 109 (1998).

[8] Swapan Das, Nucl. Phys. A **781** 509 (2007).

[9] G. E. Brown and M. Rho, Phys. Rev. Lett. **66**, 2720 (1991).

[10] E. L. Bratkovskaya, W. Cassing, M. Effenberger and U. Mosel, Nucl. Phys. A **653**, 301 (1999).

[11] Swapan Das, Phys. Rev. C **72** 064619 (2005); nucl-th/0601016.

[12] Swapan Das, Phys. Rev. C **66**, 014604 (2002).

[13] D. V. Bugg et al., Phys. Rev C **146**, 980 (1966); S. Barshay et al., Phys. Rev. C **11**, 360 (1975); W. Grein, Nucl. Phys. **B131**, 255 (1977); Particle Data Group, Phys. Rev. D **54**, 192 (1996); C. Lechanoine-Leluc et al., Rev. Mod. Phys. **65**, 47 (1993).

[14] Particle Data Group, Phys. Rev. D **54**, 576 (1996).

[15] H. De. Vries and C.W. De Jager, Atomic data and Nuclear data tables **14**, 479 (1974).

[16] M. Post, S. Leupold and U. Mosel, Nucl. Phys. **A689**, 753 (2001).

Table 1: Values for ρN resonances' parameters taken from the Ref. [7]. $L_{2I,2J}$ is the spectroscopic symbol for the pion-nucleon resonance state. S_Σ denotes the spin-isospin transition factor. All other symbols carry their usual meanings.

$R(m_R)L_{2I,2J}$	$I(J^P)$	l_ρ	Γ_π	Γ_ρ	$f_{RN\rho}$	S_Σ
$N(1520)D_{13}$	$\frac{1}{2}(\frac{3}{2}^-)$	0	95	25	7.0	8/3
$\Delta(1620)S_{31}$	$\frac{3}{2}(\frac{1}{2}^-)$	0	130	20	2.5	8/3
$N(1650)S_{11}$	$\frac{1}{2}(\frac{1}{2}^-)$	0	135	15	0.9	4
$\Delta(1700)D_{33}$	$\frac{3}{2}(\frac{3}{2}^-)$	0	180	120	5.0	16/9
$N(940)-$	$\frac{1}{2}(\frac{1}{2}^+)$	1	0	0	7.7	4
$\Delta(1232)P_{33}$	$\frac{3}{2}(\frac{3}{2}^+)$	1	120	0	15.3	16/9
$N(1680)F_{15}$	$\frac{1}{2}(\frac{5}{2}^+)$	1	118	12	6.3	6/5
$N(1720)P_{13}$	$\frac{1}{2}(\frac{3}{2}^+)$	1	50	100	7.8	8/3
$\Delta(1905)F_{35}$	$\frac{3}{2}(\frac{5}{2}^+)$	1	140	210	12.2	4/5

Table 2: Optical potentials for the ρ meson due to ρN resonance-hole polarizations in the ^{12}C nucleus. Potentials are tabulated below for the ρ meson kinetic energy $T_\rho = 1227.25$ MeV. This value corresponds to $m_\rho = 770$ MeV and $T_{p'} = 1500$ MeV.

ρN partial wave (l_ρ)	N/Δ	$V_{O\rho}$ (MeV) (Non-relativistic)	$V_{O\rho}$ (MeV) (Relativistic)
$l_\rho = 0$ (s wave)	$N(1520)$	-1.94, -11.12	-2.24, -23.95
	$\Delta(1620)$	1.24, -2.66	0.99, -4.14
	$N(1650)$	0.56, -0.52	0.51, -0.65
	$\Delta(1700)$	-0.38, -4.88	-1.20, -10.01
$l_\rho = 1$ (p wave)	$N(940)$	34.46, –	–, –
	$\Delta(1232)$	-8.57, -27.81	-1.40, -28.13
	$N(1680)$	-0.99, -4.72	-0.69, -4.89
	$N(1720)$	14.11, -33.92	6.53, -25.61
	$\Delta(1905)$	1.17, -22.74	-0.96, -20.01

Figure Captions

1. The ρ meson mass distribution spectra due to s wave ρN resonances have been compared. The non-relativistic ρ meson self-energy is used in this calculation (see text).

2. The ρ meson mass distribution spectra due to p wave ρN resonances have been compared. The non-relativistic ρ meson self-energy is used in this calculation (see text).

3. The coherent and incoherent contributions to the cross section arising from all ρN resonances are compared. The non-relativistic ρ meson self-energy is used in this calculation (see text).

4. The ρ meson mass distribution spectra due to s wave ρN resonances have been compared. The relativistic ρ meson self-energy is used in this calculation (see text).

5. The rho meson mass distribution spectra due to p wave ρN resonances have been compared. The relativistic ρ meson self-energy is used in this calculation (see text).

6. The coherent and incoherent contributions to the cross section arising from all ρN resonances are compared. The relativistic ρ meson self-energy is used in this calculation (see text).

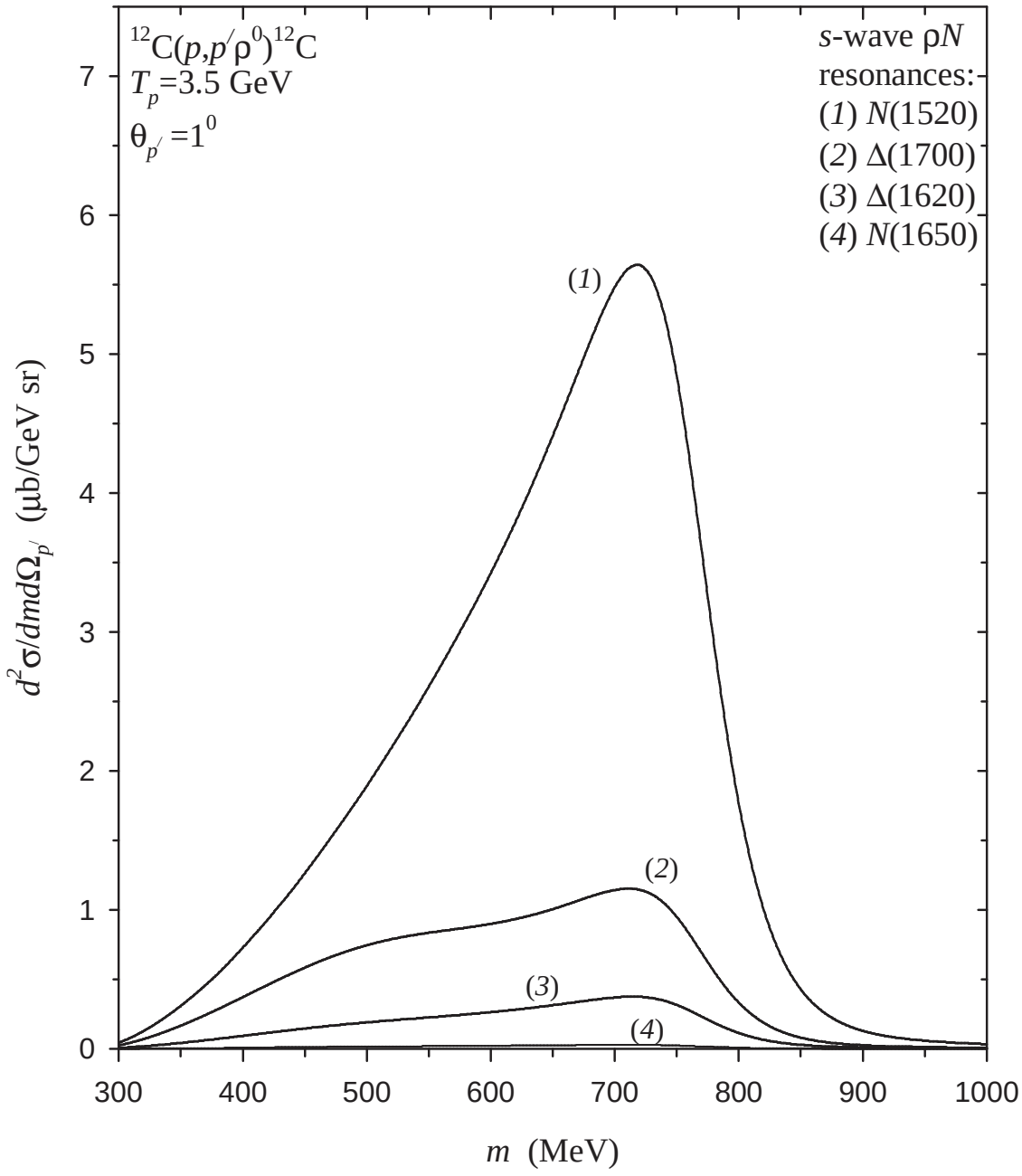

Fig.1
Author: Swapan Das

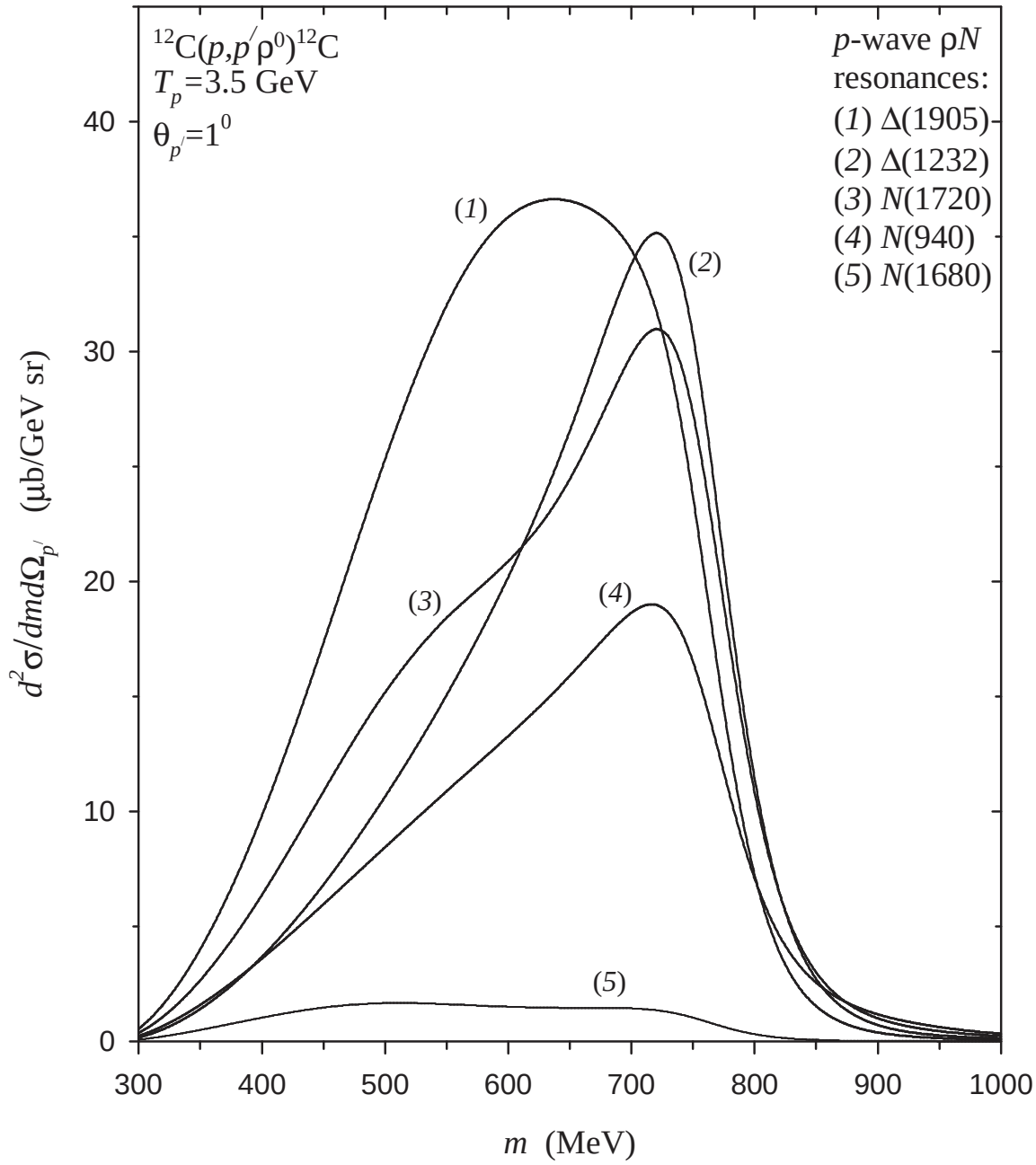

Fig.2
Author: Swapan Das

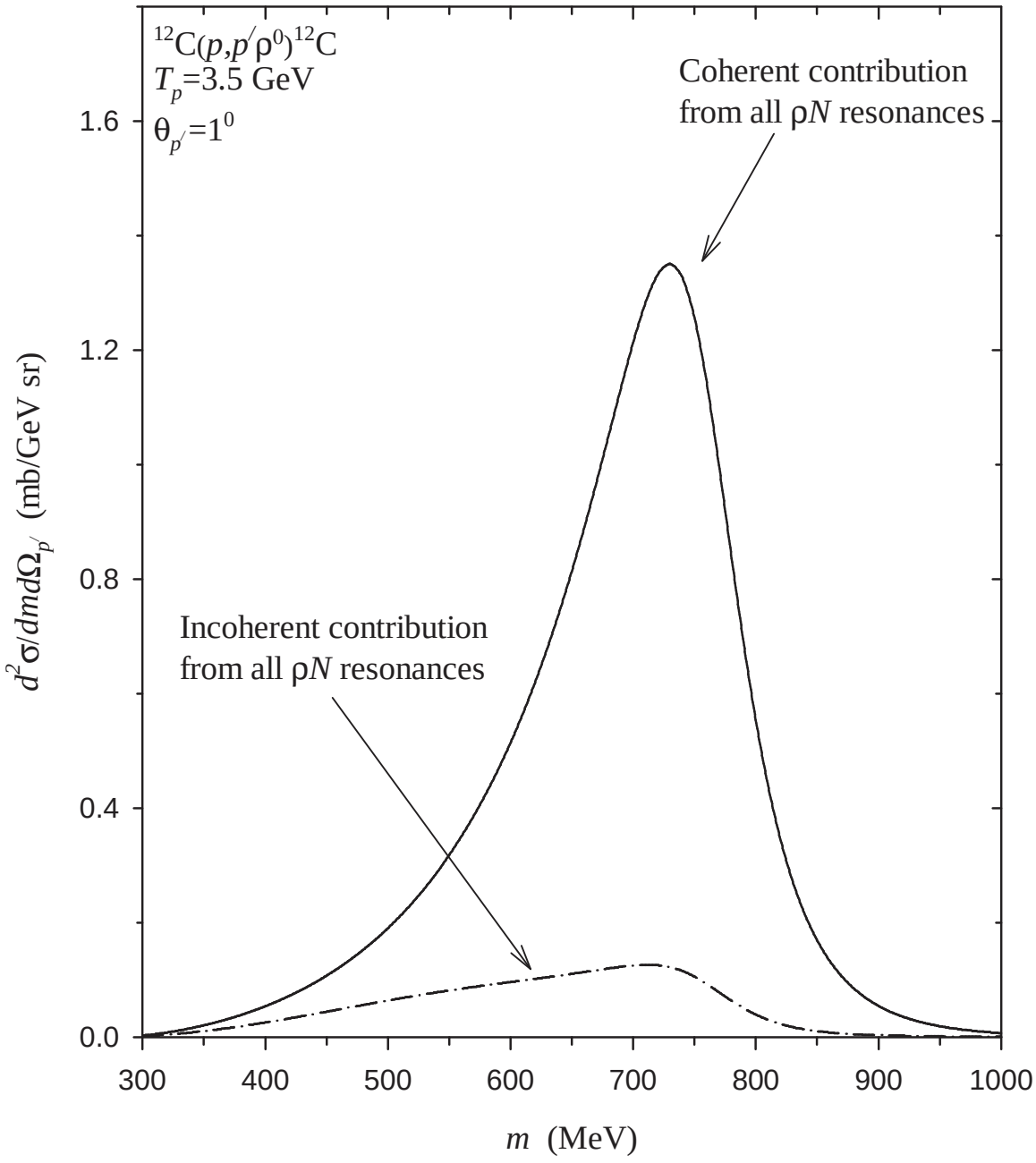

Fig.3
Author: Swapan Das

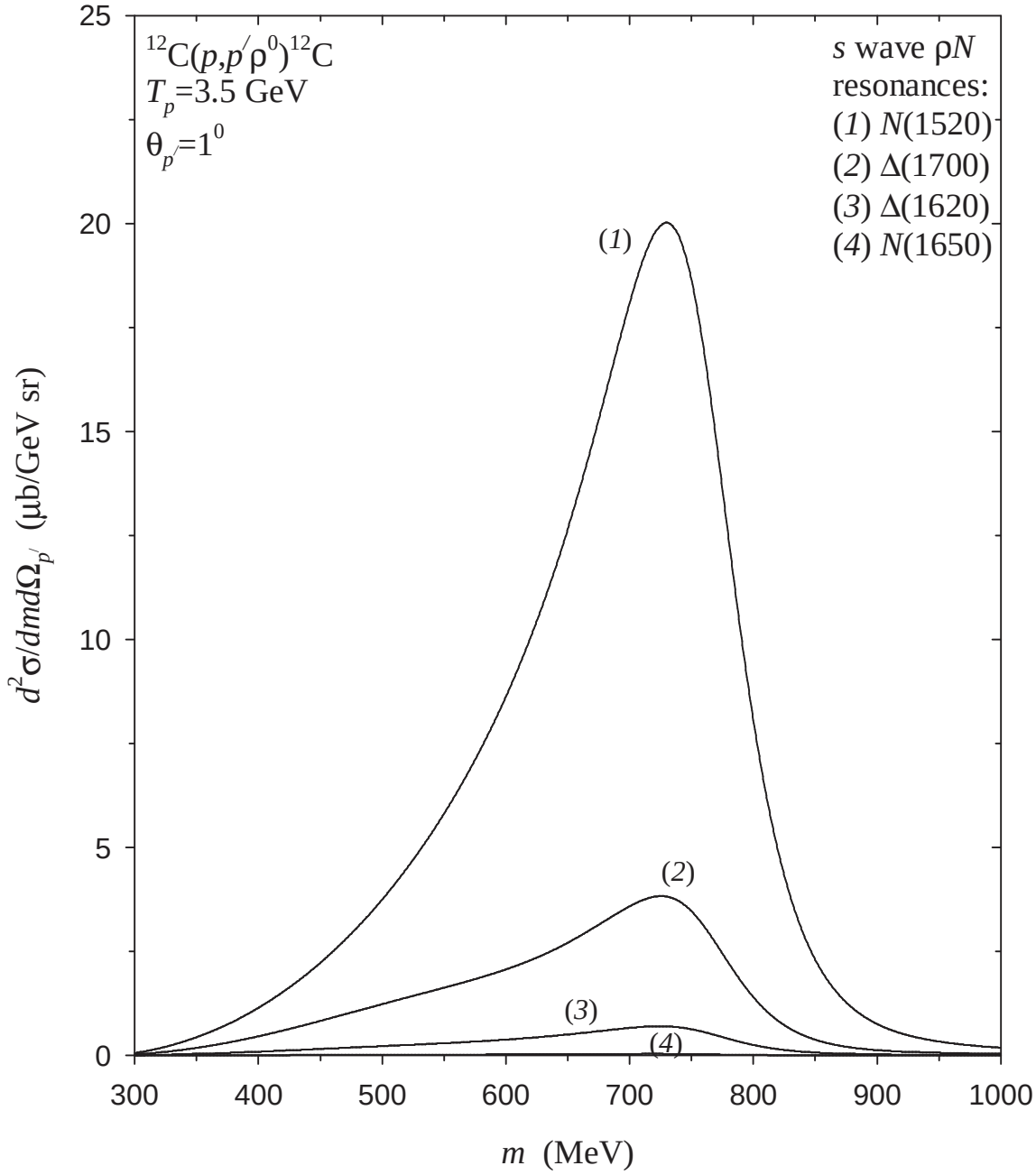

Fig.4
Author: Swapan Das

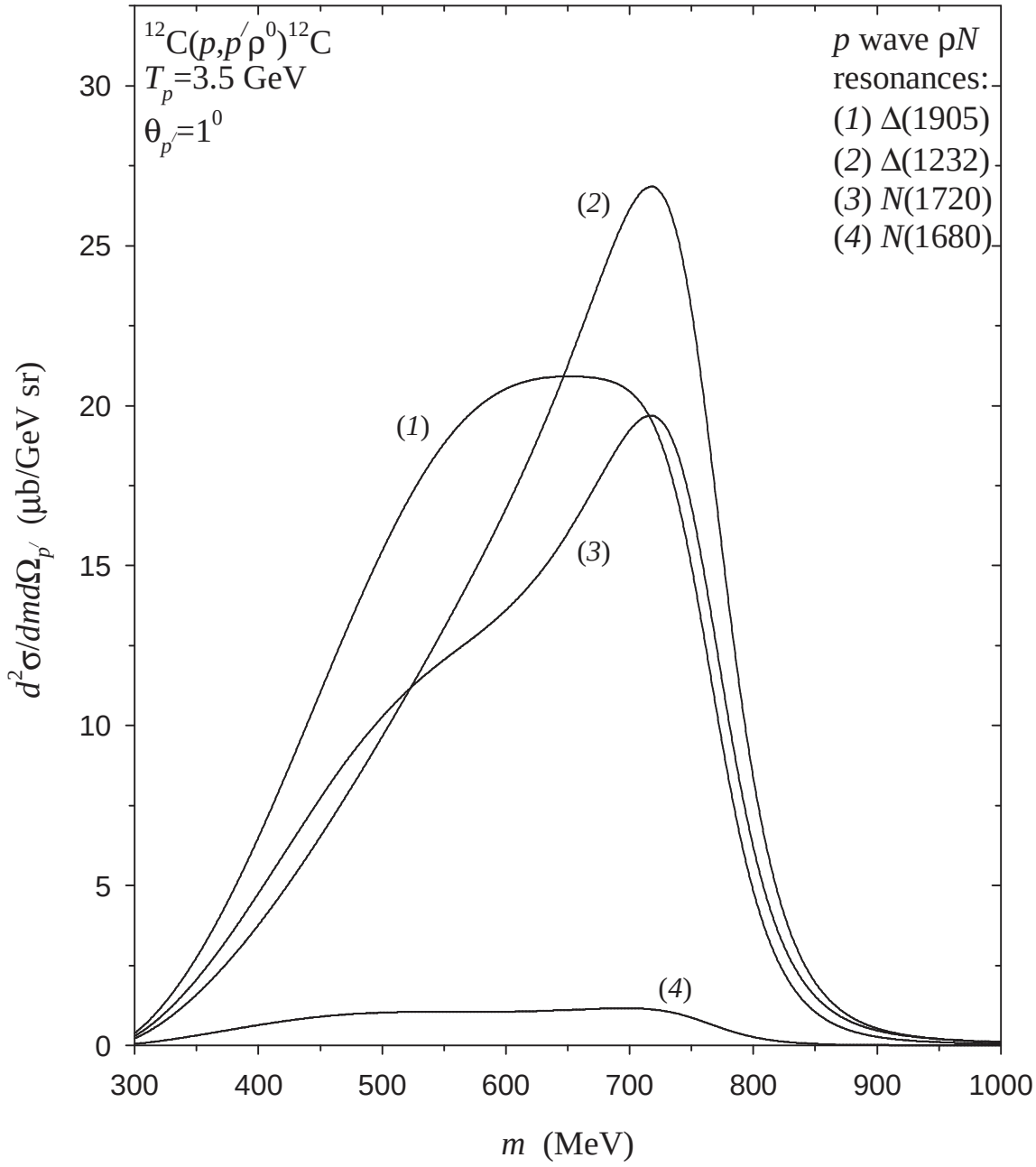

Fig.5
Author: Swapan Das

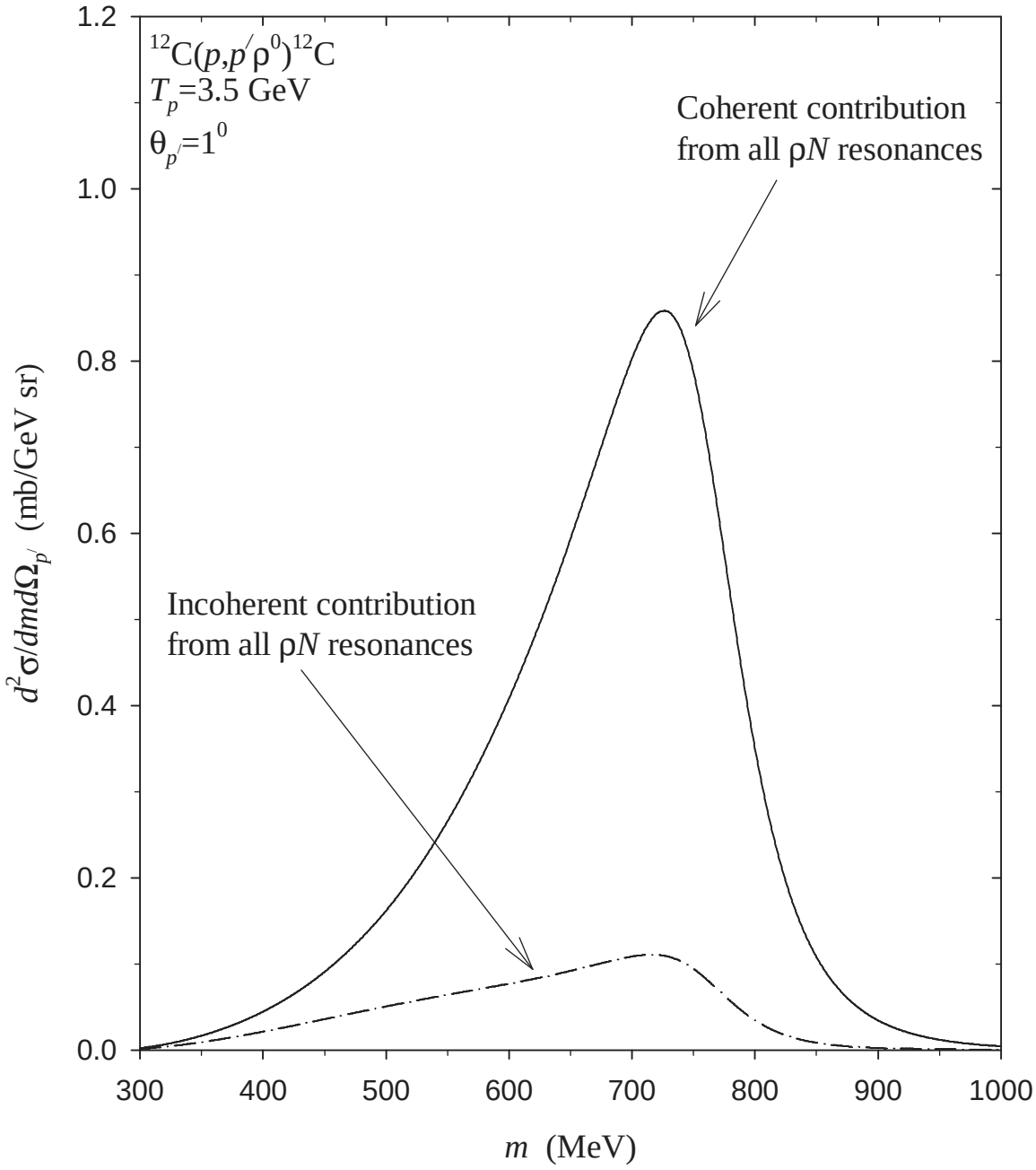

Fig.6
Author: Swapan Das